conventional α-helix with planar or nearly planar peptide units has the lowest energy. On the other hand, calculations using the Kitaigordsky function lead to the minimum for the α-helical structure, with $\Delta\omega \sim 5°$. In this minimum energy region, the helical structures have fourfold or near fourfold symmetry and pitch around 6 Å. The helix with $n = 4$ and a $5 \rightarrow 1$ hydrogen bonding scheme has been referred to as the ω-helix in the literature, but the height per residue is around 1.35 Å.[20] Though the choice is purely arbitrary, we have preferred to call the helix with $n \sim 4$ and $h \sim 1.5$ Å an α'-helix, since the h is the same as that of the conventional α-helix. In the region corresponding to average nonplanar distortion of the peptide unit observed in the crystal structures of oligopeptides containing the Aib-Aib sequence ($\Delta\omega \sim 6°$), both B and K functions lead to the α'-helix. In that region of $\Delta\omega$, the minimum for 3_{10}-helical structures attributed by the K function is within 1.5 kcal/monomer unit from that of α-helical structures. The 3_{10}-helical conformations in this minimum energy region have pitch around 6.25 Å. So, for poly(Aib) the conventional α-helix is not obligatory and an α'-helix and a 3_{10}-helix are possible, but with nonplanar distortion of the peptide unit. The electron diffraction data of poly(Aib) suggest helical structures with pitch of 6 Å, and Malcolm has interpreted the data in terms of the 3_{10}-helix, although near meridional reflection of 1.49 Å could be indicative of an α-helix.[3] We have listed all of the minimum energy helical conformations having pitch around 6 Å in Table II. All of the meridional or near-meridional reflections of the electron diffraction data, we find, can be interpreted in terms of the α'-helix. The 1.49 reflection thus fits well with the α'-helix. It is of particular interest to note that the crystal structure of Tosyl(Aib)$_5$-OMe which has been recently reported by Shamala et al.[5] showed that the pentapeptide adopts a 3_{10}-helical conformation and the average nonplanar distortion corresponds to $\Delta\omega$ around +6°. However, it should be noted that the energy difference between α'- and 3_{10}-helices (Table II) is more than compensated for by the additional hydrogen bond present in the 3_{10}-helical conformation of the pentapeptide.

We believe that further diffraction data are needed to unequivocally establish the structure of poly(Aib) as the α'-helix or the 3_{10}-helix.

Acknowledgment. We thank Professor G. N. Ramachandran for drawing our attention to this problem and Drs. P. Balaram and R. Chandrasekaran for their keen interest. Financial support from PL-480-USPHS Grant 01-126-N is acknowledged.

References and Notes

(1) Marshall, G. R.; Bosshard, H. E. *Cir. Res., Suppl.* **1972**, *30, 31*, 143.
(2) Burgess, A. W.; Leach, S. T. *Biopolymers* **1973**, *12*, 2599.
(3) Malcolm, B. R. *Biopolymers* **1977**, *16*, 2591.
(4) Nagaraj, R.; Shamala, N.; Balaram, P. *J. Am. Chem. Soc.* **1979**, *101*, 16.
(5) Shamala, N.; Nagaraj, R.; Balaram, P. *Biochem. Biophys. Res. Commun.* **1977**, *79*, 292.
(6) Shamala, N.; Nagaraj, R.; Balaram, P. *J. Chem. Soc., Chem. Commun.* **1978**, *N22*, 996.
(7) Venkataram Prasad, B. V.; Shamala, N.; Nagaraj, R.; Chandrasekaran, R.; Balaram, P. *Biopolymers* **1979**, *18*, 1635.
(8) Venkataram Prasad, B. V.; Shamala, N.; Nagaraj, R.; Balaram, P. *Acta. Crystallogr.*, in press.
(9) Smith, G. D.; Duay, W. L.; Ezerwinski, E. W.; Kendrick, N. E.; Marshall, G. R.; Mathew, F. S. "Peptides: Proceedings of the Fifth American Peptide Symposium"; Wiley: New York, 1977; p 277.
(10) Aubry, A.; Protas, J.; Bosshard, G.; Marrand, M.; Neel, J. *Biopolymers* **1978**, *17*, 1693.
(11) IUPAC-IUB Commission on Biochemical Nomenclature; *Biochemistry* **1970**, *9*, 3471.
(12) Ramachandran, G. N.; Lakshminarayanan, A. V.; Kolaskar, A. S. *Biochim. Biophys. Acta* **1973**, *303*, 8.
(13) Ramachandran, G. N.; Sasisekharan, V. *Adv. Protein Chem.* **1968**, *23*, 283.
(14) Ramachandran, G. N.; Chandrasekharan, R.; Chidambaram, R. *Proc. Indian Acad. Sci., Sect. A* **1971**, *74*, 284.
(15) Venkatachalam, C. M.; Ramachandran, G. N. "Conformation of Biopolymers"; Academic Press: New York, 1967; p 83.
(16) Ramachandran, G. N.; Chandrasekaran, R.; Chidambaram, R. *Proc. Indian Acad. Sci., Sect. A* **1971**, *74*, 270.
(17) Alok K. Mitra. *J. Indian Inst. Sci.* **1976**, *58*, 587.
(18) Flory, P. J. In "Statistical Mechanics of Chain Molecules"; Academic Press: New York, 1969; Chapter 7.
(19) Premilat, S.; Hermans, J. Jr. *J. Chem. Phys.* **1973**, *59*, 2602.
(20) Taked, Y. *Biopolymers* **1975**, *14*, 891.

Electron Spin Resonance Study of Poly(α-L-glutamic acid)– and Poly(acrylic acid)–Copper(II) Complexes in the Frozen State with Emphasis on the Complex Species [1]

Sumihare Noji and Kiwamu Yamaoka*

Faculty of Science, Hiroshima University, Higashisenda-machi, Hiroshima 730, Japan.
Received February 5, 1979

ABSTRACT: ESR spectra of Cu(II) in the presence of poly(sodium α-L-glutamate) (poly(Glu)) and poly(sodium acrylate) (poly(Acr)) were measured in frozen aqueous solutions at various degrees of neutralization (α') (0.2–1.0), pH 3–11 at room temperature, and at various molar mixing ratios of polymer residue to cupric ion (8–64). The parallel hyperfine constants, $g_\parallel$ values, line widths, and line heights of the polyanion–Cu(II) complexes were determined by means of computer simulation of the observed ESR spectra. The Cu(II)-residue complexes of two different classes (classes 1 and 2) were concluded to exist in the poly(Acr)–Cu(II) system. In the poly(Glu)–Cu(II) system, the Cu(II)-residue complex containing one ligand nitrogen atom (class *N*) was found to exist in addition to the same complexes of classes 1 and 2 as found in the poly(Acr)–Cu(II) system. The magnetic parameters of the Cu(II)-residue complexes were compared with those of Cu(II)–glutarate and –malonate complexes. The Cu(II)-complex species of $Cu(COO)_4^{2-}$ and $Cu(COO)_3^-$ were assigned to class 1 and the species of $Cu(COO)_2$ to class 2. The Cu(II)–residue complex of class *N* was found to be the Cu(NH)$(COO)_2$.

Interactions between polyelectrolytes and metal ions have been investigated from various points of view, e.g., catalytic activity[2-5] and conformational change of polymer–metal ion complexes.[6-28] In particular, polyelectrolyte–copper complexes have been utilized as model compounds to elucidate the mechanism of the biological ac-

0024-9297/79/2212-1110$01.00/0

tivity of copper proteins.[2-5,9-29] A recent study of the copper complexes of poly(L-lysine), poly(L-ornithine), and poly(L-diaminobutyric acid) (poly(A_2bu)) showed that at least a deprotonated peptide nitrogen is coordinated to a cupric ion in each complex and that the structure of the Cu(II) complexes was concluded not to be compatible with the α-helical conformation.[15]

The conformation of poly(L-glutamate) (poly(Glu)) bound by Cu(II) has been studied extensively.[17-24] A recent study has shown that two side chain carboxylato groups are coordinated to a cupric ion to induce an α-helical conformation in poly(Glu) in the pH range above 5, below which bound Cu(II) tends to dissociate.[24] Changes in both absorption and CD spectra depended on pH, which was interpreted as being due to an interplay of the coil-helix and helix-aggregate transitions of poly(Glu)-Cu(II) complexes.[24] The effect of cupric ion on the conformation of poly(Glu) appears to differ from the case of poly(Lsy), poly(Orn), and poly(A_2bu).[15] The coordination of the peptide nitrogen atom has been indicated in the poly(Glu)-Cu(II) complex;[18] yet, the α-helical structure is retained.[24] In order to elucidate the diverse effect of cupric ions on the conformational change of the Cu(II)-bound poly(amino acid)s, detailed studies on the structure of the Cu(II)-residue complex appear to be indispensable.

The local structure of polymer-Cu(II) complexes may be studied by the ESR method. ESR spectra of poly(Glu)-Cu(II) complexes showed the superhyperfine splitting which indicates the presence of one or two nitrogen atoms per cupric ion.[18] However, the pattern of the superhyperfine splitting cannot be explained solely with the interaction between Cu(II) and one or two ligand nitrogen atoms. In order to resolve the splitting of ESR spectra of poly(Glu)-Cu(II) complexes into the nitrogen superhyperfine structure, the ESR simulation of the observed spectra should be carried out. In spite of ESR studies on the Cu(II) complexes of poly- and oligopeptides,[25-28] none that resembles the ESR of poly(Glu)-Cu(II) complexes has been reported. Hence it is highly desirable, for quantitative comparison, to obtain ESR spectra of the polymer-Cu(II) complex in which the residue has a carboxyl group but no nitrogen atom. Poly(acrylate) (poly(Acr)) satisfies this requirement. Since it is known to undergo no drastic conformational change such as helix-coil transition, the poly(Acr)-Cu(II) complex can be used to clarify the effect of pH, i.e., the dissociation of the side chain carboxylate, on the structure of the Cu(II)-residue complex. The present ESR study of poly(Glu)- and poly(Acr)-Cu(II) complexes was carried out from these points of view.

Experimental Section

Materials. Poly(sodium α-L-glutamate), abbreviated simply as poly(Glu), was kindly supplied from Ajinomoto Co., Ltd. (Tokyo, Japan) and purified by dialyzing it against redistilled water for 24 h, freeze-drying, and then vacuum-drying for 7 h at 56 °C. The weight-average degree of polymerization (DP_w) was determined to be ca. 600 from the intrinsic viscosity in 2 M NaCl solution. Poly(sodium acrylate), abbreviated simply as poly(Acr), was purchased from Nakarai Chemicals Co. (Kyoto, Japan) and purified by fractional precipitation.[16,21] Its DP_w was 7700. Reagent grade malonic, glutaric, and adipic acids were used without further purification. Reagent grade copper(II) chloride dihydrate was dissolved in distilled water just prior to use.

Preparation of Sample Solutions. The stock solutions of poly(Glu) and poly(Acr) were prepared as previously described.[16,24] The molar mixing ratio of polymer residue to cupric ion (R) was controlled by varying the polymer concentration at a constant cupric ion concentration of 0.5 mM. The degree of neutralization of the carboxyl group (α') was controlled by varying the concentration of HCl ($[HCl]_{add}$) added to the sample solution. The α' was defined as $\alpha' = (C_p - [HCl]_{add})/C_p$, where C_p is the total residue concentration of polymer. In order to keep the total concentration of chloride ions nearly equal to C_p (C_p = 32, 8, and 4 mM at R = 64, 16, and 8, respectively), an appropriate amount of NaCl solution was added to the sample solution. The pH of all solutions was measured at room temperature, as described previously,[24] and noted wherever convenient to compare the ESR result of the frozen solution with other physical data at room temperature. In the study of the Cu(II)-dicarboxylate complex at low R in the frozen state, sucrose (60 mM) instead of perchlorate salts (1-2 M)[29] was added to each sample solution at a constant cupric ion concentration of 1.5 mM to avoid the formation of clusters. The oxygen was removed from the sample solution in a sample tube (5 mm in diameter) by the freeze-thaw method.

ESR Measurements. ESR spectra were measured on a JOEL Model JES-ME-3X X-band spectrometer, using a 100 kHz modulation frequency. The magnetic field was calibrated with crystalline diphenylpicrylhydrazyl (DPPH) as the standard (g = 2.0036). All spectra were taken at 77 K with a modulation width of 6.3 G.

Computer Simulation of ESR Spectra. In order to determine the number of nitrogen atoms coordinated to Cu(II), the g values, and the hyperfine and superhyperfine coupling constants, the observed spectra were simulated on a HITAC-8700 computer with a program based on a second-order perturbation theory for the calculation of ESR spectra of polycrystalline samples of the $S = {}^1/_2$ transition metal ion complexes which possess an axial symmetry.[30,31]

Since the ESR spectra of polymer-Cu(II) complexes were composed of two or more component spectra (vide post), the heights and positions of lines in the $g_\perp$ region were complicated. The estimation of both the g_x and g_y values and hyperfine coupling constants of A_x and A_y was impractical. Thus, the spectra were simulated in detail in the $g_\parallel$ region which was hardly affected by the variation of both the $g_\perp$ values (2.09-2.05) and the perpendicular hyperfine coupling constants (8-25 G). The individual line shape function was taken to be Gaussian. The observed spectra of poly(Acr)- and poly(Glu)-Cu(II) complexes showed the variations in line widths with the spin quantum number of copper nucleus (vide post). Therefore, the line width parameters (ΔH_m) of the line shape function were adjusted in such a way that a good agreement results between the observed and simulated spectra. Here, m is the spectral index number of the mth hyperfine line from the low magnetic field side. The starting set of the parameters involved in simulation was adjusted by the trial-and-error method until the best possible fit was obtained.

Results and Discussion

ESR Spectra of Poly(Acr)-Cu(II) Complexes. Typical ESR spectra of poly(Acr)-Cu(II) complexes at three R values are shown in Figure 1. The spectrum at R = 64 is clearly a composite of two different spectra of Cu(II) complexes which have different parallel hyperfine coupling constants ($A_\parallel$), as indicated by 1 and 2 in Figure 1. For the sake of convenience, the complex (or a mixture of slightly differing complexes) of one class which gives a larger $A_\parallel$ value was termed class 1 and the other class was termed class 2. The presence of the Cu(II)-aquo complex may be excluded, since almost all cupric ions are bound to the polymer sites in this α' or pH range at room temperature.[16,23] Thus, the Cu(II)-Acr residue complexes of classes 1 and 2 are formed in the poly(Acr). The $A_\parallel$ and $g_\parallel$ values estimated by computer simulation are listed in Table I. The ESR spectrum at R = 16 also shows the presence of Cu(II)-Acr complexes of the same classes as those at R = 64. The spectrum at R = 8 was so broad that the number of Cu(II)-Acr complexes was not determined. Since ESR spectra became broader with the decrease in R, the well-resolved ESR spectra at R = 64 were analyzed in detail.

Figure 2 shows the $g_\parallel$-region ESR spectra of poly(Acr)-Cu(II) complexes at R = 64 and 16 and at various values of α'. A broad spectrum emerges at the smallest α' of 0.2, as indicated by 3. The spectrum indicates that

Table I
The $A_{\parallel}$ and $g_{\parallel}$ Values of Poly(Glu)-, Poly(Acr)-, Glutarate-, and Malonate-Cu(II) Complexes at 77 K

poly(Glu)-Cu(II)					poly(Acr)-Cu(II)				
R	α' (pH)	class[a]	$A_{\parallel}$[b]	$g_{\parallel}$[c]	R	α' (pH)	class	$A_{\parallel}$	$g_{\parallel}$
64-16	0.2-1.0	1	151	2.328	64-16	0.4-1.0	1	155	2.330
	(4.55-7.14)	2	144	2.355		(4.72-7.42)	2	135	2.365
		N[d]	153	2.330					
64	(11.9)[e]	N	195	2.191					

Cu(II)-glutarate					Cu(II)-malonate				
R	pH	species[f]	$A_{\parallel}$	$g_{\parallel}$	R	pH	species	$A_{\parallel}$	$g_{\parallel}$
80	4.8	1′	160	2.326	80	4.3	1′	158	2.329
		2′	143	2.354	4	5 2	1′	158	2.329
4	5.5	2′	144	2.366	2	5.8	2′	149	2.362
2	5.2	3′	124	2.418	2	3.9	3′	124	2.418

[a] The class of Cu(II)-residue complexes (see text for details). [b] The experimental uncertainty is ±2 G. [c] The experimental uncertainty is ±0.005. [d] The parallel superhyperfine coupling constant is 25-26 G. [e] An aqueous NaOH solution was added instead of HCl. [f] Complex species (see text for details).

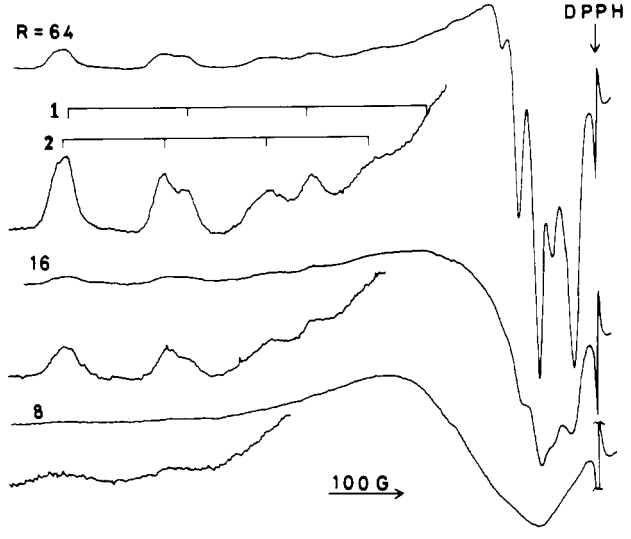

Figure 1. ESR spectra of poly(Acr)–Cu(II) complexes at 77 K, at R = 64, 16 and 8, and at α' = 1.0 (pH 7.4–7.6). The $g_{\parallel}$ region is shown at a 3.4-fold increased gain. The parallel hyperfine lines of Cu(II)–Acr complexes which belong to two classes (1 and 2) are indicated by (⊔⊔). The microwave frequency is 9.24 GHz.

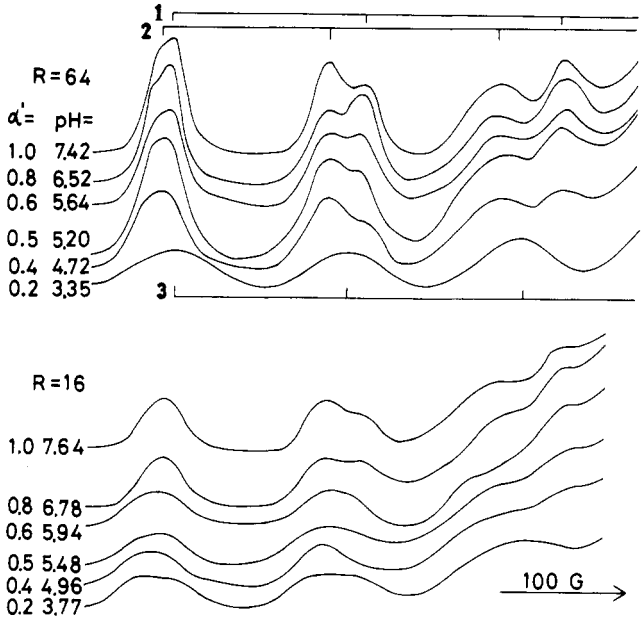

Figure 2. The $g_{\parallel}$ regions of the ESR spectra for poly(Acr)–Cu(II) complexes at R = 64 and 16 and at 77 K in the α' range 0.2–1.0. Other conditions are the same as those in Figure 1.

this complex differs from the Cu(II)–Acr complexes of classes 1 and 2, but may involve a cluster of Cu(II) dissociated from poly(Acr).[16] The relative heights of the second hyperfine lines of classes 1 and 2 vary with α', but the positions of the lines remain almost unaltered with α' except at the smallest α'. (The hyperfine lines are numbered from the low magnetic field side.) Thus, the α' dependence of the ESR spectra at R = 64 and 16 reflects the variation of the concentrations of the complex species of classes 1 and 2 with α'.

In order to determine the line widths and line heights of the component ESR spectrum of each class at various α', the observed R = 64 spectra were simulated. The $g_{\parallel}$ regions of the best-fitted simulation spectra are shown in Figure 3. The results show that the line widths of the hyperfine lines or the ΔH_m values of the observed spectra depend on α' and the spectral index number m. These values are given in the caption of Figure 3. The dependence of ΔH_m on m in the ESR spectra of the poly(Acr)–Cu(II) complexes may result from the inhomogeneous distribution of ligand field, as previously noted for the Co(II)–dimethylglyoxime complex at 77 K in the frozen state.[32]

ESR Spectra of Poly(Glu)–Cu(II) Complexes. Figure 4 shows the typical ESR spectra of poly(Glu)–Cu(II) complexes at three R values. The R = 64 spectrum differs from the corresponding spectrum of poly(Acr)–Cu(II) complex in that, at least, four and three superhyperfine lines can be observed in the first and second hyperfine lines, respectively. This splitting is probably due to the peptide nitrogen atom coupled with Cu(II).[18] On the other hand, no superhyperfine line is discernible in the R = 8 ESR spectrum. The ESR spectra were broadened with decrease in R; hence, the well-resolved ESR spectra at R = 64 were analyzed below.

Figure 5 shows the $g_{\parallel}$ regions of the ESR spectra. The variation with α' is distinctly different from the case of the poly(Acr)–Cu(II) complex in Figure 2. Although the relative heights of the superhyperfine lines vary with α' in a complicated manner, the number of lines for the complexes of higher R values (R = 64–16) remains unchanged in the α' range 0.3–0.8: four superhyperfine lines in the first hyperfine line and three or four in the second one. This implies that the dominant species of Cu(II)–Glu complexes remain unaltered in the α' range 0.2–0.8, even if the R values vary from 64 to 16. Thus, the α' dependence of the ESR spectra is attributed to the change in the relative concentrations of the chemical species with the protonation of the carboxylato group of poly(Glu).

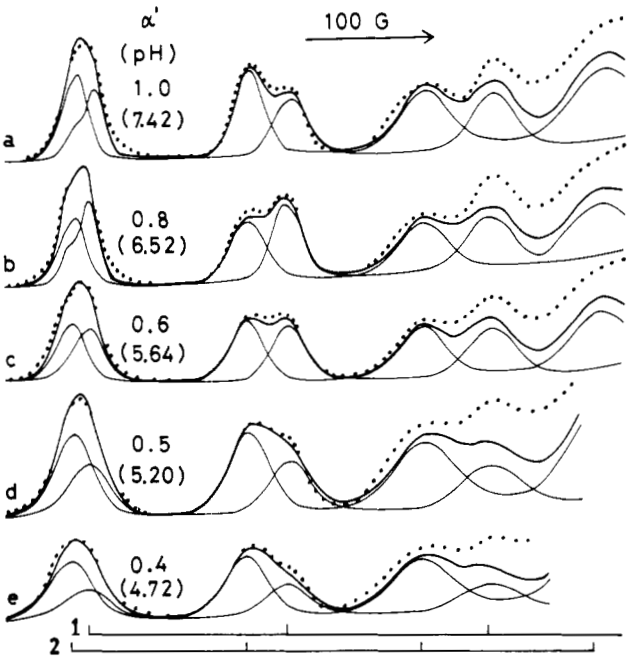

Figure 3. The simulated $g_{\parallel}$ regions of the ESR spectra for a poly(Acr)–Cu(II) complex at R = 64 in the α' range 0.4–1.0. The solid curves denote both the simulated component and resultant spectra. The natural abundance of the ^{63}Cu(II) and ^{65}Cu(II) isotopes was strictly taken into account in computing the component spectra of classes 1 and 2. See text for details. The dotted curves denote the observed spectra at various α'. (a) α' = 1.0 (pH 7.42), ΔH_1 = 14 and 16, ΔH_2 = 26 and 22, and ΔH_3 = 32 and 38 for classes 1 and 2, respectively; (b) α' = 0.8 (pH 6.52), ΔH_1 = 13 and 16, ΔH_2 = 22 and 26, and ΔH_3 = 38 and 36; (c) α' = 0.6 (pH 5.64), ΔH_1 = 20 and 20, ΔH_2 = 26 and 26, and ΔH_3 = 36 and 36; (d) α' = 0.5 (pH 5.20), ΔH_1 = 26 and 26, ΔH_2 = 32 and 32, and ΔH_3 = 46 and 46; (e) α' = 0.4 (pH 4.72), ΔH_1 = 30 and 30, ΔH_2 = 33 and 33, and ΔH_3 = 46 and 46 (ΔH_m is expressed in G). The vertical lines at the bottom of the Figure indicate the positions of hyperfine lines of the ^{63}Cu(II) complexes of classes 1 and 2. The magnetic parameters are listed in Table I.

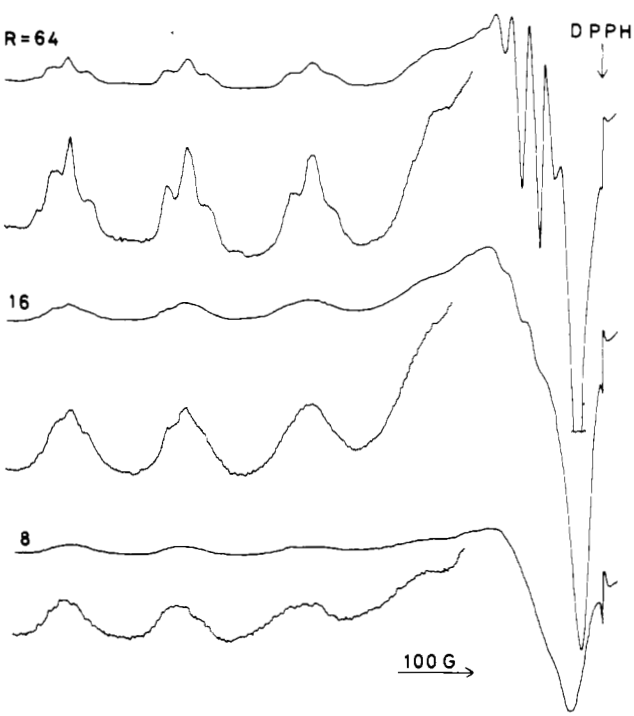

Figure 4. ESR spectra of poly(Glu)–Cu(II) complexes at 77 K, at R = 64, 16, and 8, and at α' = 0.3, 0.5, and 0.5 (pH 5–6), respectively. Other conditions are the same as those in Figure 1.

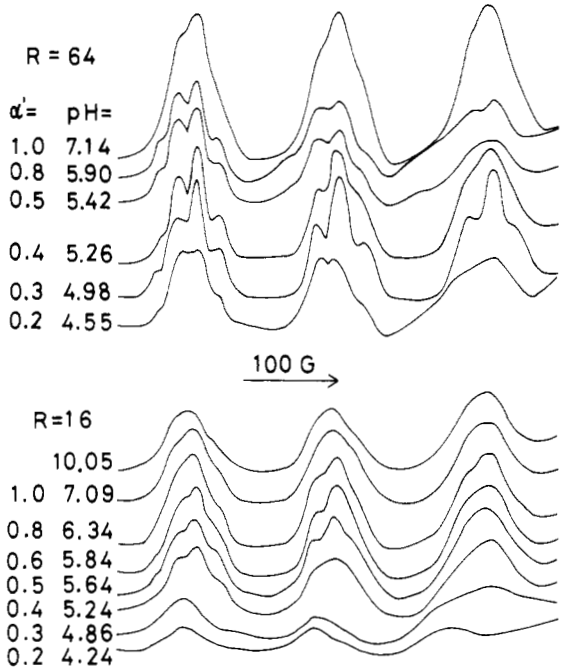

Figure 5. The $g_{\parallel}$ regions of the ESR spectra for poly(Glu)–Cu(II) complexes at R = 64 and 16, at 77 K, and at various α'. Other conditions are the same as those in Figure 1.

The lowest-field line in the first hyperfine line has been attributed to the first superhyperfine line of the isotope ^{65}Cu(II) complex in the mixed isotope spectrum.[33] Appearance of four superhyperfine lines in the first line implies that the number of the superhyperfine lines belonging to each of isotopes ^{63}Cu(II) and ^{65}Cu(II) should be three rather than five in the α' range 0.3–0.8. Hence, the number of the ligand nitrogen atoms coordinated to each Cu(II) is one rather than two. (If the latter were the case, five superhyperfine lines should have been observed.[33]) The relative line heights of three superhyperfine lines from one ligand nitrogen atom should be 1:1:1 theoretically. However, the observed relative line heights not only differ from the theoretical ratio but also depend on α'. This indicates the presence of Cu(II)–Glu complexes of various classes in addition to the complex which contains a nitrogen atom as the ligand. Since the apparent $A_{\parallel}$ values of the Cu(II)–Glu complexes are nearly equal to those of the Cu(II)–Acr complexes of classes 1 and 2, the observed ESR spectra of poly(Glu)–Cu(II) should be composed of the component spectra of the class 1 and class 2 complexes in addition to a component spectrum of a nitrogen-containing Cu(II) complex.

The observed ESR spectra of poly(Glu)–Cu(II) complexes at R = 64 were simulated by taking into account the natural abundance and the hyperfine coupling constant of ^{65}Cu(II). (A hyperfine coupling constant of the ^{65}Cu(II) complex is larger by 1.07 than that of the ^{63}Cu(II) complex.[33]) When a complex was assumed to contain two equivalent ligand nitrogen atoms, the number of the simulated superhyperfine lines disagreed with the observed one. Hence, the absence of a Cu(II)–Glu complex, which involves two ligand nitrogen atoms, was assured. When three-component spectra, those of classes 1 and 2 and of the complex containing one ligand nitrogen atom, were superimposed, a good agreement was obtained between the observed and simulated spectra. The best simulated spectra are shown in Figure 6. Here, the values of $A_{\parallel}$ and $g_{\parallel}$ for classes 1 and 2 were slightly modified. The values of $g_{\parallel}$, $A_{\parallel}$, and the superhyperfine coupling constant are listed in Table I. The ΔH_m values are given in the caption

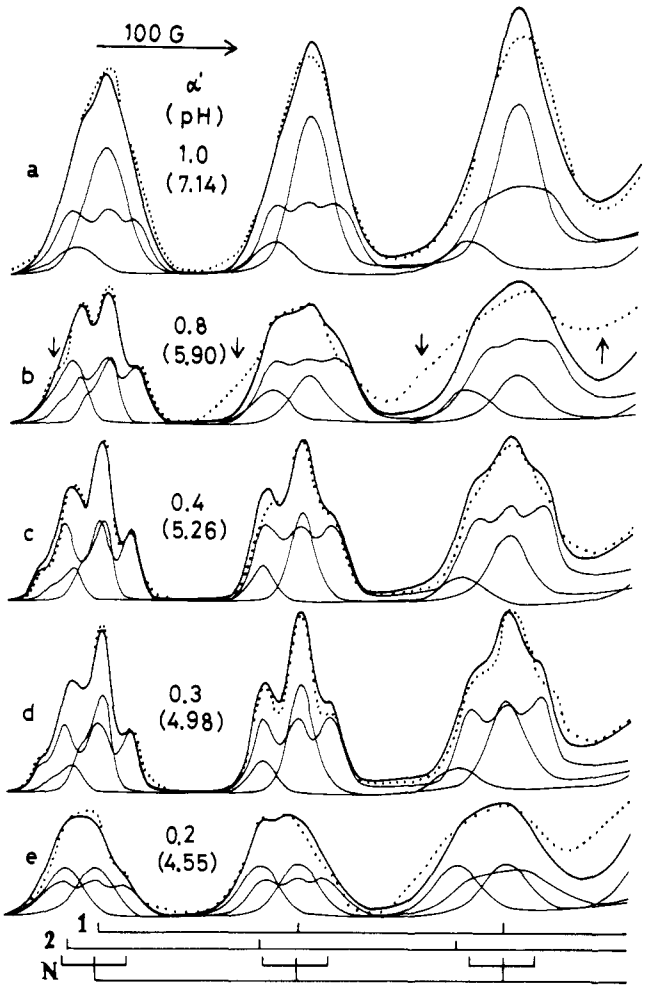

Figure 6. The simulated $g_{\parallel}$ regions of the ESR spectra for a poly(Glu)–Cu(II) complex at $R = 64$ in the α' range 0.2–1.0. The solid curves denote both the simulated component and resultant spectra. The natural abundance of the ^{63}Cu(II) and ^{65}Cu(II) isotopes was strictly taken into account in computing the component spectra of classes 1, 2, and N. See text for details. The dotted curves denote the observed spectra at various α'. (a) $\alpha' = 1.0$ (pH 7.14), $\Delta H_1 = 28$, 28, and 18, $\Delta H_2 = 28$, 28, and 21, and $\Delta H_3 = 33$, 33, and 33 for classes 1, 2, and N, respectively; (b) $\alpha' = 0.8$ (pH 5.90), $\Delta H_1 = 13$, 13, and 15, $\Delta H_2 = 24$, 24, and 22, and $\Delta H_3 = 28$, 28, and 33; (c) $\alpha' = 0.4$ (pH 5.26), $\Delta H_1 = 13$, 13, and 12, $\Delta H_2 = 24$, 18, and 18, and $\Delta H_3 = 28$, 30, and 22; (d) $\alpha = 0.3$ (pH 4.98), $\Delta H_1 = 13$, 13, and 13, $\Delta H_2 = 18$, 18, and 16, and $\Delta H_3 = 28$, 28, and 20; (e) $\alpha' = 0.2$ (pH 4.55), $\Delta H_1 = 23$, 23, and 18, $\Delta H_2 = 28$, 28, and 21, and $\Delta H_3 = 33$, 33, and 30 (ΔH_m is expressed in G). The vertical lines at the bottom of the figure indicate the positions of the hyperfine and superhyperfine lines for the ^{63}Cu(II) complexes of classes 1, 2, and N. Arrows indicate four hyperfine lines of a minor and unidentified Cu(II) complex. The magnetic parameters are listed in Table I.

of Figure 6. The class of Cu(II)–Glu complexes, which contain a nitrogen atom, is termed class N. It should be noted that a Cu(II)–Glu complex, which belongs to neither class 1, 2, or N, is present in the $R = 64$ poly(Glu)–Cu(II) at a very high pH of 11. This is a "biuret complex" and is termed the class N' complex. The $g_{\parallel}$ and $A_{\parallel}$ values for class N' are also given in Table I.

ESR Spectra of Cu(II)–Complexes with Low Molecular Weight Model Compounds. In order to determine structures of Cu(II)–residue complexes classified by classes 1 and 2, the ESR spectra of the Cu(II) complexes with malonate and glutarate were measured in the frozen solution. The results are shown in Figure 7. The Cu(II)–glutarate complex at $R = 80$ (pH 4.8) gave rise to the ESR spectrum which closely resembles that of the poly-

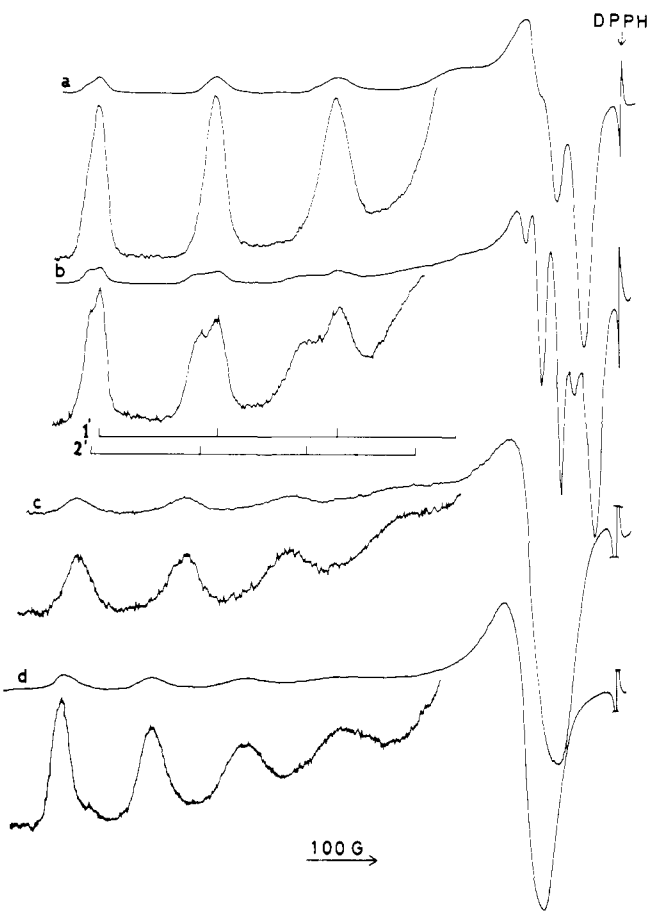

Figure 7. ESR spectra of (a) the Cu(II)–malonate complex at $R = 80$ (pH 4.3) and of (b, c, d) the Cu(II)–glutarate complexes at $R = 80$ (pH 4.8), 4 (pH 5.5), and 2 (pH 5.2), respectively, at 77 K. The $g_{\parallel}$ region is expanded by a six- to sevenfold gain. The parallel hyperfine lines of two species of Cu(II)–glutarate complexes at $R = 80$ are indicated by (⊔⊔).

(Acr)–Cu(II) complex obtained under similar conditions (cf. Figure 7b and Figures 1 and 2). The Cu(II)–adipate complex at $R = 80$ (pH 4.8) also showed the spectrum very similar to that of the Cu(II)–glutarate complex: Both spectra consist of two components. On the contrary, the Cu(II)–malonate complex at any R gave rise to a single-component ESR spectrum under the same condition (Figure 7a). The Cu(II)–glutarate complexes at $R = 4$ and 2 (pH ca. 5.5) both showed the single-component ESR spectrum which, however, differs from that of the Cu(II)–malonate complex at $R = 80$ as regards the $A_{\parallel}$ and $g_{\parallel}$ values (c and d in Figure 7). The $A_{\parallel}$ and $g_{\parallel}$ values of these complexes are given in Table I. Two Cu(II)–glutarate complex species at $R = 80$ are termed species 1′ and 2′ from the higher magnetic field side. They correspond to classes 1 and 2 of the Cu(II)–Acr complexes. The $A_{\parallel}$ and $g_{\parallel}$ values of species 1′ are nearly equal to those of the Cu(II)–malonate complexes at $R = 80$ and 4, while the $A_{\parallel}$ and $g_{\parallel}$ values of species 2′ are close to those of the Cu(II)–glutarate complex at $R = 4$ and Cu(II)–malonate at $R = 2$ (pH 5.8). Since the structure of the Cu(II)–malonate complexes has been reported to be Cu(–COO)$_2$ at an R of about 2[34,35] and Cu(–COO)$_4^{2-}$ at an R higher than 4,[36] the Cu(–COO)$_4^{2-}$ and Cu(–COO)$_2$ complexes can be assigned to the species 1′ and 2′ and, hence, to classes 1 and 2, respectively. A third species (species 3′) was observed in the spectra of the Cu(II)–glutarate complex at $R = 2$ and the Cu(II)–malonate complex at $R = 2$ and at pH 3.9. It may be assigned to Cu(–COO)$^+$ on the basis of their $A_{\parallel}$ and $g_{\parallel}$ values, which differ from those of the Cu(II)–aquo

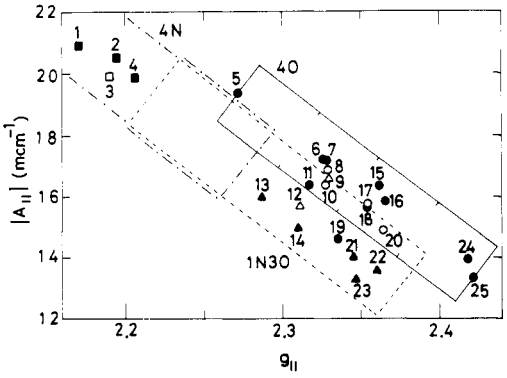

Figure 8. The $|A_{\parallel}|$ vs. $g_{\parallel}$ correlation diagram for the Cu(II) complexes of four-oxygen ligation (4O) (○), one-nitrogen and three-oxygen ligation (1N3O) (△), and four-nitrogen ligation (4N) (□). Open symbols are for polymer–Cu(II) complexes, while filled symbols are for low molecular weight compound–Cu(II) complexes. The areas enclosed by (—), (- - -) and (-·-) indicate the expected limits of the ESR parameters for 4O, 1N3O and 4N ligations, respectively.[38] Numerals are as follows: (1) for $(Gly)_3$ at pH 10.1;[27] (2) for acetylglycylglycyl-L-histidylglycine at pH 11;[28] (3) for class *N'* (poly(Glu)); (4) for acetylglycyl-L-hystidylglycine at pH 11;[28] (5) for $Cu(OH)_4^{2-}$;[29] (6) for species **1'** (glutarate); (7) for species **1'** (malonate); (8) for class 1 (poly(Acr)); (9) for class *N* (poly(Glu)); (10) for class 1 (poly(Glu)); (11) for $Cu(oxalate)_2^{2-}$;[37] (12) for transferrin–bicarbonate $^{63}Cu(II)$;[45] (13) for $(Gly)_3$ at pH 4.5;[27] (14) for $(Gly)_4$ at pH 4.5;[26] (15) for species **2'** (malonate); (16) for species **2'** (glutarate); (17) for class 2 (poly(Glu)); (18) for species **2'** (glutarate) at $R = 80$; (19) for poly(Acr) at $\alpha' = 0.2$; (20) for class 2 (poly(Acr)); (21) for $(Gly)_3$ at pH 4;[26] (22) for $(Gly)_2$ at pH 4;[26] (23) for $(Gly)_3$ at pH 3;[26] (24) for species **3'** (glutarate and molonate); and (25) for $Cu(H_2O)_4^{2+}$.[37]

complex.[37]

Cu(II)-Residue Complexes in Poly(Acr)- and Poly(Glu)-Cu(II) Macroions. In order to assign the specific structure to each Cu(II)-residue complex in poly(Acr) and poly(Glu), the $A_{\parallel}$ and $g_{\parallel}$ values of the Cu(II)-residue complexes were compared with those of the low molecular weight Cu(II) complexes. The $A_{\parallel}$ values are plotted against the $g_{\parallel}$ values for various classes and species in Figure 8. Peisach and Blumberg[38] have pointed out that the placement of a negative charge on a five-atom core of a Cu(ligand)$_4$ can decrease the $g_{\parallel}$ value but increase the $A_{\parallel}$ value. For the four-oxygen ligation (4O), compounds with varying charges on the core lie inside the area enclosed by solid lines in Figure 8. A dipositive complex (No. 25), $Cu(H_2O)_4^{2+}$, is located in the lower right of the area, while a dinegative complex (No. 5), $Cu(OH)_4^{2-}$, is located in the upper left. As the net charge on the five-atom core (4O + Cu) of a complex varies from +2 to −2, the point of this complex should move in the $A_{\parallel}$ vs. $g_{\parallel}$ plot almost linearly in the 4O area according to its charge.[38] Thus, a structural assignment of a given Cu(II) complex can be made on the basis of its position in the $A_{\parallel}$ vs. $g_{\parallel}$ plot.

The points of the class 1 complexes (No. 8 and 10 for poly(Acr)- and poly(Glu)-Cu(II), respectively) are located near the points of the species 1' complexes (No. 6 and 7 for the Cu(II)-glutarate and -malonate complexes of Cu(-COO)$_4^{2-}$ type, respectively) and the $Cu(oxalate)_2^{2-}$ complex (No. 11). Thus, a structure of the Cu(II)-residue complexes of class 1 should be Cu(-COO)$_4^{2-}$ (species **1a** of Figure 9, where one of the resonance states is described). The positions of these complexes in the 4O area indicate that the net charge of the five-atom core is about −0.5. If four acidic oxygen atoms interact with a cupric ion, the net charge might be −2. The net charge of −0.5 may, therefore, result from some electronic interaction of one or both of the keto oxygen atoms with the cupric ion in the class 1 complex. The Cu(-COO)$_3^-$ complex may also

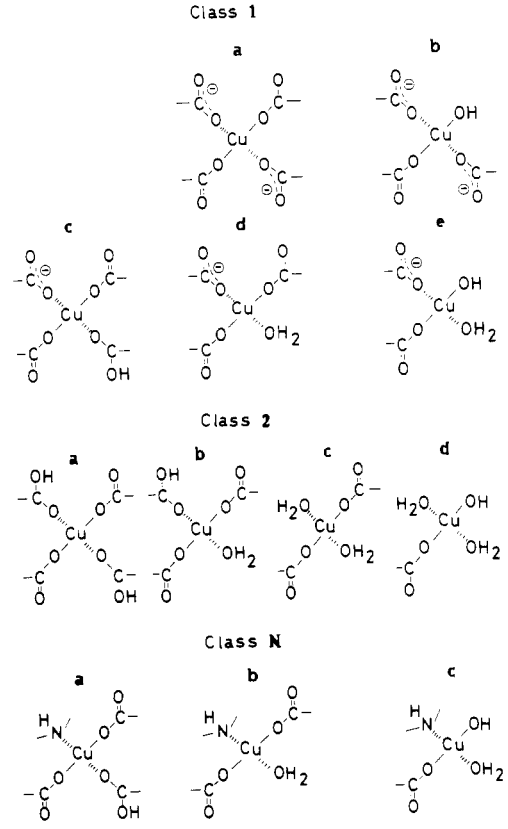

Figure 9. The possible structures of Cu(II)–residue complexes formed in poly(Acr)- and poly(Glu)–Cu(II) macroions. Structures a–e represent individual chemical species. The trans configurations of the ionized carboxylates are shown, although the cis configurations are also possible.

be assigned to class 1 on the same basis as is advanced for the Cu(-COO)$_4^{2-}$ complex. The possible structure of the Cu(-COO)$_3^-$ species is the species **1c** or **1d** in Figure 9.

The plausible structures for the Cu(II)–Glu and -Acr complexes of class 2 are the species **2a**, **2b**, and **2c** in Figure 9, because the points of poly(Glu)–Cu(II) (No. 17) and poly(Acr)–Cu(II) (No. 20) of class 2 are located near the points of the species **2'** complexes of Cu(II)–malonate (No. 15) and of Cu(II)–glutarate (No. 16 and 18) in the 4O area, and because a cupric ion neutralizes at least two carboxylato groups in both poly(Glu)- and poly(Acr)–Cu(II) systems.[23]

The one-nitrogen and three-oxygen ligation (1N3O) has been characterized only incompletely, because no well-defined example whose five-atom core has a negative net charge has been found.[38] (The area is enclosed by dashed lines in Figure 8.) However, the position of the Cu(II)–Glu complex of class *N* (No. 9) is located in the middle of the area of 1N3O. This indicates that the net charge of the class *N* complex may be nearly zero. Hence, the complex of class *N* probably contains at least two carboxylato groups in addition to a peptide nitrogen atom. The Cu(II)–peptide complexes generally show the visible absorption bands below 600 nm, when the deprotonated peptide nitrogen atom is involved.[15] However, the Cu(II)–Glu complexes of class *N* can be concluded to contain the protonated peptide nitrogen atom, since the visible absorption band appears near 700 nm.[24] Thus, the most plausible structure for class *N* may be species ***N*a** or ***N*b**. For comparison, the point of the Cu(II)–Glu complex of class *N'*, i.e., "biuret complex", is plotted in Figure 8 (No. 3). This point falls near the group of other biuret-like complexes (No. 1 for triglycylglycine–Cu(II), No. 2 for acetylglycylglycyl-L-histidylglycine–Cu(II), and No. 4 for

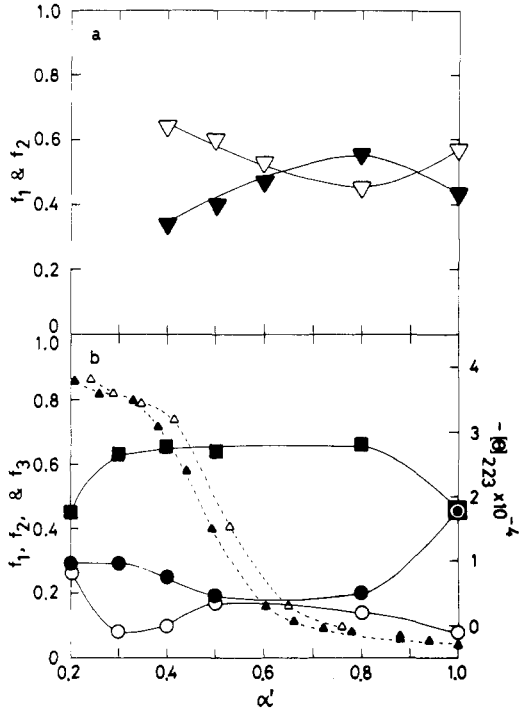

Figure 10. The α' dependence of the fractions of (a) classes 1 (-▼-) and 2 (-▽-) in the poly(Acr)-Cu(II) system at R = 64 and (b) classes 1 (-●-), 2 (-○-), and N (-■-) in the poly(Glu)-Cu(II) system at R = 64. The helix-coil transition is shown, for comparison, with the molar ellipticity ($[\theta]_{223}$) of poly(Glu) (--▲--) and of poly(Glu)-Cu(II) complex at R = 32 (--△--) at room temperature.[24]

acetylglycyl-L-histidylglycine-Cu(II)) in the area of four-nitrogen ligation (4N).

Effect of α' on Complex Formation in the Poly(Acr)-Cu(II) Systems. The ratio of the concentration of the class 1 Cu(II)-Acr complex to that of the class 2 (β) was estimated in the frozen state from the area of the first hyperfine peak of the simulated component spectrum.[25] Fractions of classes 1 and 2 ($f_1 = \beta/(1+\beta)$ and $f_2 = 1/(1+\beta)$) were estimated under the assumption that $f_1 + f_2 = 1$ and are plotted against α' in Figure 10a. With the decrease in α' from 0.8 to 0.4 (pH 6.52-4.74), the value of f_1 decreases; thus, the dominant species **1a**, **1c**, and **1d** of class 1 (Figure 9) may transform to species **2a**, **2b**, and **2c** of class 2. On the other hand, the value of f_2 is larger than that of f_1 at α' = 1 (pH 7.42). This reverse trend may indicate the participation of a hydroxide ion in complex formation,[16] as shown by species **1b** and **1e** of class 1 or **2d** of class 2 in Figure 9. (A hydroxide ion cannot be distinguished from a charged oxygen atom on the basis of ESR parameters.)

Complex formation between poly(Acr) and Cu(II) has been investigated by potentiometric[23,39,40] and optical titration.[16,41] The finding that the dominant species in the poly(Acr)-Cu(II) system is $Cu(-COO)_2$[23] is consistent with the presence of $Cu(-COO)_4^{2-}$, because potentiometric titration is insensitive to differentiate them.[23] In fact, it has been suggested from absorption spectroscopic studies that $Cu(-COO)_4^{2-}$ is formed in the poly(methacrylate)-Cu(II)[39] and poly(Acr)-Cu(II)[16] systems.

The formation of a binuclear Cu(II) complex of the acetate type, in which the direct Cu(II)-Cu(II) interaction exists, in the poly(methacrylate)-Cu(II) complex has been deduced on the basis of the appearance of a shoulder at about 370 nm in the absorption spectra.[42] The poly(Acr)-Cu(II) complexes also show the 370-nm band most remarkably at low pH near 4.5 regardless of R.[16] Nonetheless, the hyperfine structures of the ESR spectrum of the poly(Acr)-Cu(II) complex at R = 16 (pH 4.96) were well resolved as shown in Figure 2. It should be noted, in this connection, that an ESR spectrum of a binuclear Cu(II) complex, e.g., the Cu(II) chelate of *N,N'*-diglycylethylenediamine, is broad and reveals no hyperfine structure.[43] Thus, the ESR spectra of poly(Acr)-Cu(II) complexes give no supporting evidence for the formation of a binuclear Cu(II)-Acr complex, as a dominant species, in the R range 64-16 and in the α' range 0.2-1.0 in the frozen state.

Effect of α' on Complex Formation in the Poly(Glu)-Cu(II) System. Fractions of the Cu(II)-Glu complexes of classes 1, 2, and N (f_1, f_2, and f_N) in the R = 64 poly(Glu)-Cu(II) system were estimated similarly to those in the poly(Acr)-Cu(II) except for the Cu(II)-Glu complex of class N. They are plotted against α' in Figure 10b. The f_N was calculated, as a rough approximation, from the triple area of the first superhyperfine peak instead of the area of the first hyperfine peak. The molar ellipticity at 223 nm, ($[\theta]_{223}$), of the poly(Glu) and Cu(II) complex at R = 32 is also shown in Figure 10b.[24] The poly(Glu) backbones undergo the helix-coil transition in the α' range 0.3-0.7 at room temperature.[24] The transition region of poly(Glu) has been reported to shift slightly toward larger α' (between 0.4 and 0.8 at 0.6 °C) with the decrease in temperature.[44] Thus, the transition region is probably in the range of 0.4-0.8 even in frozen solutions, provided that the conformation of poly(Glu)-Cu(II) complexes is retained by freezing.

In the α' range 0.2-0.3 where the CD data showed that both poly(Glu) and poly(Glu)-Cu(II) form aggregates at room temperature,[24] the f_2 increases, while the f_N decreases. This result indicates that the species ***N*b** changes to the species **2a**, **2b**, and **2c** of class 2 rather than to the species ***N*a** in the helical poly(Glu) aggregates probably because of spacial restrictions imposed upon it by such aggregate formation. On the other hand, Cu(II)-Glu complexes of class 1 seem to transform partially to those of class N with the decrease in α' from 1.0 to 0.8, where the poly(Glu)-Cu(II) complex may be in the coiled form. In this region, the presence of species **1b**, **1e**, and ***N*c** could not be excluded, however. Many Cu(II)-Glu complexes of slightly different structures may also be present, because the observed ESR spectrum at α' = 1 is extremely broad (see the caption of Figure 6).

It is of interest to note that the formation of helix does not affect the fraction of Cu(II)-Glu complexes of class N. This means that the species ***N*b** may be compatible with the α-helical backbone of the Cu(II)-bound poly(Glu) at larger R values, provided that the helical conformation remains in the frozen solution. The coordination of a peptide nitrogen atom has been found in the Cu(II) complexes of poly(Lys), poly(Orn), and poly(A_2bu), in which the structure of the Cu(II)-residue complexes was not compatible with the α-helical backbone.[15] However, this is not the case for the poly(Glu)-Cu(II) complex because the helical conformation is induced by the bound Cu(II).[24] The helix of poly(Glu)-Cu(II) should be stabilized by the binding of at least two side-chain carboxylates per Cu(II) as shown in Figure 9 (except for the species **1b**, **1e**, **2d**, and ***N*c**).

The present work has clarified that the interaction between the cupric ion and the carboxylate-containing poly(Glu) and poly(Acr) leads to the formation of a large number of Cu(II)-residue complexes and that the interplay of these complex species results in the complicated pH (or α') dependence of the ESR spectra. The present ESR

method should also be applicable to other polyelectrolyte–Cu(II) systems. The results no doubt help us to interpret the optical absorption data of the same systems less ambiguously.

Summary

The local structure of poly(Acr)- and poly(Glu)–Cu(II) macroions could be estimated in frozen solutions by the ESR method. The plausible structures of Cu(II)-residue complexes in poly(Acr)- and poly(Glu)–Cu(II) are summarized as follows. For poly(Acr)–Cu(II): (1) The Cu(II)–Acr complexes of species **1a**, **1c**, **1d**, **2a**, **2b**, and **2c** all involving either two, three, or four side-chain carboxylates are formed in the α' range of 0.4–1.0. (2) The complex species of **1b**, **1e**, and **2d** may be formed near $\alpha' = 1.0$ (in the pH range above 7). For poly(Glu)–Cu(II): (1) The Cu(II)–Glu complexes of species **1a**, **1c**, **1d**, **2b**, and ***N*b** prevail in the coil region (α' 0.8–1.0 or pH 6–7), and in addition, the species **1b**, **1e**, **2d**, and ***N*c** may also be present. (2) In the helix–coil transition region, the complexes of species **1a**, **1c**, **1d**, **2b**, **2c**, and ***N*b** are predominant. The structure of species ***N*b** seems to be compatible with the α-helical backbone at least in the R range 16–64. (3) In the helix–aggregate region (α' 0.2–0.3), the complexes of species **1a**, **1c**, **2a**, **2b**, and ***N*b** are preferentially formed. The complexes of **1a**, **1c**, and **2a** may be formed between two or more helical strands.

References and Notes

(1) This is Macromolecules–Metal Ion Complexes. 7. For the previous paper of this series, see ref 24.
(2) Y. Moriguchi, *Bull. Chem. Soc. Jpn.*, **39**, 2656 (1966).
(3) H. Sigel and G. Blauer, *Helv. Chim. Acta.* **51**, 1246 (1968).
(4) A. Levitzki, I. Pecht, and A. Berger, *J. Am. Chem. Soc.*, **94**, 6844 (1972).
(5) M. Hatano and T. Nozawa, *Prog. Polym. Sci. Jpn.*, **4**, 223 (1972).
(6) A. L. Jacobson, *Biopolymers*, 1, 269 (1963).
(7) N. Kono and A. Ikegami, *Biopolymers*, 4, 823 (1966).
(8) O. Iwaki, K. Hikichi, M. Kaneko, S. Shimizu, and T. Maruyama, *Polym. J.*, 4, 623 (1973).
(9) M. Hatano, T. Nozawa, S. Ikeda, and Y. Yamamoto, *Makromol. Chem.*, **141**, 1 (1971).
(10) T. Nozawa and M. Hatano, *Makromol. Chem.*, **141**, 21 (1971).
(11) A. Garnier and L. Tosi, *Biopolymers*, 14, 2247 (1975).
(12) N. Hojo, K. Fukatsu, and T. Hayakawa, *Nippon Kagaku Zasshi*, **90**, 823 (1969).
(13) M. Kawai, T. Hayakawa, and N. Hojo, *Nippon Kagaku Zasshi*, **92**, 617 (1971).
(14) M. Palumbo, A. Cosani, M. Terbojevich, and E. Peggion, *J. Am. Chem. Soc.*, **99**, 939 (1977).
(15) M. Palumbo, A. Cosani, M. Terbojevich, and E. Peggion, *Macromolecules*, **10**, 813 (1977).
(16) K. Yamaoka and T. Masujima, *Bull. Chem. Soc. Jpn.*, **52**, 1819 (1979).
(17) A. L. Jacobson, *Biopolymers*, **2**, 207 (1964).
(18) H. Takesada, H. Yamazaki, and A. Wada, *Biopolymers*, **4**, 713 (1966).
(19) Y. Hibino and S. Sugai, *Rep. Prog. Polym. Phys. Jpn.*, **11**, 513 (1968).
(20) S. Inoue, K. Yamaoka, and M. Miura, *Bull. Chem. Soc. Jpn.*, **44**, 1443 (1971); **45**, 1314 (1972); *J. Sci. Hiroshima Univ. Ser. A*, **39**, 27 (1975).
(21) K. Yamaoka and T. Masujima, *Polym. J.*, in press.
(22) S. Yamashoji, H. Yoshida, and G. Kajimoto, *Yukagaku*, **25**, 128 (1976).
(23) J. A. Marinsky, *Coord. Chem. Rev.*, **19**, 125 (1976).
(24) K. Yamaoka and T. Masujima, *Bull. Chem. Soc. Jpn.*, **52**, 1286 (1979).
(25) T. Vänngård in "Biological Applications of Electron Spin Resonance", H. M. Swartz, J. R. Bolton, and D. C. Borg, Eds., Wiley, New York, 1972, pp 411–447.
(26) T. H. Crawford and J. O. Dalton, *Arch. Biochem. Biophys.*, **131**, 123 (1969).
(27) K.-E. Falk, H. C. Freeman, T. Jansson, B. G. Malmström, and T. Vänngård, *J. Am. Chem. Soc.*, **89**, 6071 (1967).
(28) G. F. Bryce, *J. Phys. Chem.*, **70**, 3549 (1966).
(29) K.-E. Falk, E. Ivanova, B. Roos, and T. Vänngård, *Inorg. Chem.*, **9**, 556 (1970).
(30) L. D. Rollmann and S. I. Chan, *J. Chem. Phys.*, **50**, 3416 (1969).
(31) J. Chen, M. Abkowitz, and J. H. Sharp, *J. Chem. Phys.*, **50**, 2237 (1969).
(32) A. Rockenbauer and P. Simon, *J. Magn. Reson.*, **18**, 320 (1975).
(33) J. S. Taylor and J. E. Coleman, *J. Biol. Chem.*, **248**, 749 (1973).
(34) D. I. Stock and C. W. Davies, *J. Chem. Soc.*, 1371 (1949).
(35) J. M. Peacock and J. C. James, *J. Chem. Soc.*, 2233 (1951).
(36) H. L. Riley, *J. Chem. Soc.*, 1642 (1930).
(37) F. A. Walker, H. Sigel, and D. B. McCormick, *Inorg. Chem.*, **11**, 2756 (1972).
(38) J. Peisach and W. E. Blumberg, *Arch. Biochem. Biophys.*, **165**, 691 (1974).
(39) A. M. Kotliar and H. Morawetz, *J. Am. Chem. Soc.*, **77**, 3692 (1955).
(40) H. P. Gregor, L. B. Luttinger, and E. M. Loeble, *J. Phys. Chem.*, **59**, 34 (1955).
(41) F. T. Wall and S. J. Gill, *J. Phys. Chem.*, **58**, 1128 (1954).
(42) J. C. Leyte, L. H. Zuiderwerg, and M. van Reisen, *J. Phys. Chem.*, **72**, 1127 (1968).
(43) T. D. Smith and A. E. Martell, *J. Am. Chem. Soc.*, **94**, 4123 (1972).
(44) D. S. Olander and A. Holtzer, *J. Am. Chem. Soc.*, **90**, 4549 (1968).
(45) R. Aasa and P. Aisen, *J. Biol. Chem.*, **243**, 2399 (1968).

Random-Coil Configurations of Polymeric Chains with Sulfur and Oxygen Atoms in Their Structure: Dipole Moments of Poly(1,3-dioxa-6-thiocane)

E. Riande* and J. Guzmán

Instituto de Plásticos y Caucho, Madrid-6, Spain. *Received May 25, 1979*

ABSTRACT: Dielectric measurements were carried out on solutions of poly(1,3-dioxa-6-thiocane) in benzene over the range of 20–60 °C. The dipole moment ratio of this chain has a value of 0.42 in the vicinity of 25 °C, which increases moderately with increasing temperature. Conformational energies arising from first-order interactions between sulfur and oxygen atoms were obtained by analysis of the dipole moments in terms of the rotational isomeric state theory of chain configurations. The present study indicates that intramolecular interactions involving S and O atoms have higher energy in gauche than in trans states, in agreement with the results found in previous studies on the configurational properties of poly(thiodiethylene) glycol.

The rapidly growing interest in elucidating structure–property relationships for polymeric systems has encouraged the study of the molecular configurations which is central to an understanding of the physical properties of any type of polymeric chains. The multitude of possible configurations, generated by different conformational sequences, gives a polymeric material the unique properties that set it off so distinctively from any low molecular

0024-9297/79/2212-1117$01.00/0